Contrasting silencing mechanisms of the same target mRNA by two regulatory RNAs in *Escherichia coli*

David Lalaouna[*], Karine Prévost, Guillaume Laliberté, Vincent Houé and Eric Massé[*]

Department of Biochemistry, RNA Group, Université de Sherbrooke, Sherbrooke, Québec, Canada

ABSTRACT

Small RNAs are key components of complex regulatory networks. These molecules can integrate multiple cellular signals to control specific target mRNAs. The recent development of high-throughput methods tremendously helped to characterize the full targetome of sRNAs. Using MS2-affinity purification coupled with RNA sequencing (MAPS) technology, we reveal the targetomes of two sRNAs, CyaR and RprA. Interestingly, both CyaR and RprA interact with the 5′-UTR of *hdeD* mRNA, which encodes an acid-resistance membrane protein. We demonstrate that CyaR classically binds to the RBS of *hdeD*, interfering with translational initiation. We identified an A/U-rich motif on *hdeD*, which is bound by the RNA chaperone Hfq. Our results indicate that binding of this motif by Hfq is required for CyaR-induced degradation of *hdeD* mRNA. Additional data suggest that two molecules of RprA must bind the 5′-UTR of *hdeD* to block translation initiation. Surprisingly, while both CyaR and RprA sRNAs bind to the same motif on *hdeD* mRNA, RprA solely acts at the translational level, leaving the target RNA intact. By interchanging the seed region of CyaR and RprA sRNAs, we also swap their regulatory behavior. These results suggest that slight changes in the seed region could modulate the regulation of target mRNAs.

INTRODUCTION

From the human intestinal tract to plant roots, bacteria face a plethora of harmful environmental factors. The nature of encountered factors can be abiotic (e.g. temperature, pH) or biotic (e.g. antibiotics, host immune system). To survive and persist in their ecological niche, bacteria have developed a mighty arsenal of sensing systems called two-component systems (TCS). Generally, TCS are composed of a membrane-associated sensor histidine kinase (HK) and a response regulator (RR) (1). For example, *Escherichia coli* genome harbors 30 HK and 32 RR (2), enabling to integrate multiple signals and to efficiently respond to stressful conditions. Indeed, in response to specific stimuli, the HK autophosphorylates and then transfers the phosphoryl group to the cognate RR. This last step of phosphorylation activates the RR. In *E. coli*, the vast majority of RRs are DNA-binding transcription factors (2). A perfect example is the CpxAR two-component system that responds to envelope stress by controlling the transcription of dozens of genes including two small regulatory RNAs (sRNAs) called CyaR and RprA (3,4).

Since the discovery of sRNAs in the early 80's, accumulated results showed the prime importance of these post-transcriptional regulators in every aspect of bacterial physiology (5). Generally, sRNAs regulate multiple target mRNAs through imperfect base-pairing in the vicinity of the ribosome binding site (RBS). By steric hindrance, sRNAs prevent the binding of the translational machinery and protein synthesis. This is generally followed by passive or active mRNA decay orchestrated by specific ribonucleases such as RNase E (6).

CyaR sRNA (cyclic AMP-activated RNA) was previously shown to negatively regulate a broad spectrum of targets such as *ompX* (7,8), *yqaE*, *nadE*, *luxS* (9) and *yobF* mRNAs (10). The expression of CyaR is quite complex as it is controlled by various effectors. Indeed, CyaR is regulated by cAMP-CRP and is subject to catabolite repression (11). Moreover, CyaR expression is also regulated by the CpxAR two-component system and presumably by the alternative sigma factor σE (3,7).

In concert with three other sRNAs, RprA positively regulates the general stress sigma factor σS (12). In addition, RprA negatively controls the transcriptional factor CsgD and the diguanylate cyclase YdaM, key factors in biofilm formation (13). In *Salmonella*, RprA inhibits the conjugation of pSLT, a virulence plasmid, via the activation of RicI translation (14). The expression of *rprA* is induced during the stationary phase of growth by the RcsCDB phosphorelay and the CpxAR two-component system (3,15). The transcription of RprA is also repressed by the global regulator of flagellar synthesis LrhA (16).

*To whom correspondence should be addressed. Tel: +1 819 821 8000 (Ext. 75475); Email: eric.masse@usherbrooke.ca
Correspondence may also be addressed to David Lalaouna. Email: david.lalaouna@usherbrooke.ca
Present address: Vincent Houé, Institut Pasteur, Department of Virology, Arboviruses and Insect Vectors, Paris, France.

Both CyaR and RprA sRNAs are involved in complex regulatory networks. In 2015, our group used MS2-affinity purification coupled with RNA sequencing (MAPS) technology to characterize three sRNA targetomes (17,18). Here, we performed MAPS to reveal the targetomes of CyaR and RprA sRNAs. While our data expand the targetomes of these sRNAs, we noticed that an acid-resistance membrane protein called HdeD is under the control of both CyaR and RprA. To understand this apparent functional redundancy, we investigated the sRNA-dependent regulatory mechanism that occurs on *hdeD* mRNA. We provided evidence that, surprisingly, two molecules of RprA are required to block the translational initiation of *hdeD*. In stark contrast, CyaR classically binds to the RBS of *hdeD* mRNA to regulate *hdeD* at both post-transcriptional and translational levels. Our results suggest that Hfq binding on target mRNA may be a prerequisite for the formation of a sRNA/mRNA/Hfq/RNase E quaternary complex.

MATERIALS AND METHODS

Strains and growth conditions

All experiments used derivatives of *E. coli* MG1655 strain (Supplementary Table S1). Cells were grown in rich medium (LB). Ampicillin was used at a final concentration of 50 μg/ml and chloramphenicol at 30 μg/ml, as needed.

RNA extraction and northern blot analysis

Total RNA was extracted following the hot-phenol protocol described by Aiba *et al.* (19). 0.1% arabinose was added when indicated to induce gene expression from the pBAD vector.

For northern blot analysis, 5–10 μg of total RNA were loaded on a polyacrylamide gel (5–10% acrylamide 29:1, 8 M urea) or 20 μg on an agarose gel (1%, MOPS 1×). Then, RNA was electro-transferred to a Hybond-XL membrane (Amersham Bioscience) for a polyacrylamide gel or transferred by capillarity on a Biodyne B membrane (Pall) for an agarose gel. Cross-linking was performed by UV (1200 J). Prehybridization was performed in Church buffer (20). Radiolabeled DNA probes used in this study are described in Supplementary Table S2. Membranes were then exposed to phosphor storage screens and analyzed using a Typhoon Trio (GE Healthcare) instrument. Results reported here correspond to data from at least two independent experiments.

MS2-affinity purification coupled with RNAseq

The MS2 aptamer was fused to the 5′end of *cyaR* and *rprA* gene. To validate MS2-sRNA constructs, we first verified that they are expressed at a level similar to untagged sRNA (control). Then, we compared its activity with the control by northern blot analysis (Supplementary Figure S1). To purify the maximum of target mRNAs, we used a Δ*sRNA rne131* (RNA degradosome assembly mutant) strain.

Affinity purification assays were performed as described in Lalaouna *et al.* (21). Here, cells were grown in LB supplemented with 50 μg/ml ampicillin (diluted 1/1000 from an overnight culture grown) and harvested (after induction with 0.1% arabinose for 10 min) in exponential ($OD_{600 nm}$ = 0.5; 100 ml) and stationary phase of growth ($OD_{600 nm}$ = 1.5; 100 ml) for MS2-CyaR and only in stationary phase of growth ($OD_{600 nm}$ = 1.5; 100 ml) for MS2-RprA.

cDNA libraries were prepared using ScriptSeq™ v2 RNA-Seq Library Preparation Kit (Illumina) and sequenced with Illumina MiSeq. Data processing was performed according to Lalaouna *et al.* (21). Most highly co-purified targets are presented in Tables 1 and 2. Reads alignment were visualized using Genome Browser (Supplementary Figures S2 and S3) (22). The whole list of genes enriched is also available in Supplementary Table S3.

β-Galactosidase assays

β-Galactosidase assays were performed as previously described (23). When required, expression of respective sRNAs was induced by addition of 0.1% arabinose at an $OD_{600 nm}$ = 0.5 (LB medium 37°C). When the cells reached an $OD_{600 nm}$ of 2, specific β-galactosidase activity was calculated using the formula $V_{max}/OD_{600 nm}$. Data represent the mean of three independent experiments (± standard deviation, SD). See Supplementary Figure S4 and Supplementary Materials and Methods for details on the construction of *lacZ* fusions.

Probing experiments

Lead acetate degradation and In-line probing assays were performed as described by Lalaouna *et al.* (18). In brief, 0.2 μM of *in vitro*-generated *hdeD*+195 5′-end-labeled was incubated with or without 1 μM CyaR or RprA sRNA. Radiolabeled RNA was incubated 5 min at 90°C with alkaline buffer or 5 min at 37°C with ribonuclease T1 (0.1 U; Ambion) to generate the alkaline (OH) ladder and the T1 ladder, respectively. RNA was analyzed on an 8% acrylamide/7 M urea gel.

RESULTS

CyaR sRNA targetome revealed by MAPS

As previously performed for RyhB, RybB and DsrA sRNAs (17,18), we used the MAPS approach to uncover the targetome of CyaR sRNA. The MS2-CyaR construct was expressed from a pBAD promoter by addition of 0.1% arabinose in an *rne131* Δ*cyaR* background. Then, we co-purified all interacting RNAs in both exponential ($OD_{600 nm}$ = 0.5) and stationary ($OD_{600 nm}$ = 1.5) phases of growth. Processed data are available in Supplementary Table S3. We summarize most enriched candidates in Table 1 and show reads alignment visualized using Genome Browser (22) in Supplementary Figure S2.

In addition to the five previously characterized targets of CyaR, we found four new candidates (i.e. *yacL*, *mgrB-yebO*, *hdeD* and *nhaA-nhaR*). Briefly, *yacL* mRNA encodes a conserved cytoplasmic protein of unknown function. Both *mgrB* and *yebO* mRNAs are transcribed as a single polycistronic transcript: while MgrB is described as a negative regulator of PhoQP two-component system (24), the function of YebO protein is still unknown. The *hdeD* mRNA encodes a membrane protein involved in high-density acid

Table 1. Characterization of CyaR targetome using MAPS technology

Gene	Ratio MS2-CyaR/Ctrl	Function/activity	Reference
yacL	370	Conserved protein	This study
mgrB	339	Regulator of the PhoQP system	This study
hdeD	199	Acid-resistance membrane protein	This study
nhaA	160	$Na^+:H^+$ antiporter	This study
luxS	108	*S*-ribosylhomocysteine lyase	De Lay, 2009
yebO	93	Hypothetical protein	This study
yqaE	70	Putative membrane protein	De Lay, 2009
yobF	38	Stress response protein	Wright, 2013
nadE	37	NAD synthetase	De Lay, 2009
ompX	32	Outer membrane protein	Johansen, 2008
nhaR	7	$Na^+:H^+$ antiporter regulator	This study

List of most significantly co-purified mRNAs using MS2-CyaR as bait in an *rne131 ΔcyaR* background (ratio MS2-CyaR/CyaR control). New putative target mRNAs are highlighted in gray. Only reads on gene sequences are reported here. The complete list of candidates is available in Supplementary Table S3.

Table 2. Identification of potential RprA-regulated mRNAs using MAPS technology

Gene	Ratio MS2-RprA/Ctrl	Function/Activity	Reference
nlpD	2295	Divisome associated factor	Majdalani, 2001
grcA	1803	Pyruvate formate-lyase subunit	This study
hdeD	1655	Acid-resistance membrane protein	This study
rpoS	1528	σS factor ($σ^{38}$)	Majdalani, 2001
focA	1101	Formate transporter	This study
lrhA	744	Transcriptional regulator	This study
pal	569	Subunit of TolB-Pal complex	This study
tolB	324	Subunit of TolB-Pal complex	This study
cpoB	103	Cell division coordinator	This study
csgD	23	Transcriptional regulator	Mika, 2012
ydaM	21	Diguanylate cyclase	Mika, 2012

List of most significantly co-purified mRNAs using MS2-RprA as bait in an *rne131 ΔrprA* background (ratio MS2-RprA/RprA control). New putative target mRNAs are highlighted in gray. Only reads on gene sequences are reported here. The complete list of candidates is available in Supplementary Table S3.

resistance (25). Finally, NhaA is an Na+:H+ antiporter involved in cellular salt and pH homeostasis and NhaR is its associated transcriptional regulator (26). Notably, those putative targets of CyaR were not previously predicted by in silico analysis or identified by microarray assays (9,10).

To validate these four potential targets of CyaR, we pulse-expressed CyaR *in vivo*, and used northern blot assays for detection (Supplementary Figures S5A and Figure 1A). We observed a rapid decrease for all target mRNAs, suggesting that CyaR negatively regulates these mRNAs at the post-transcriptional level. To further characterize CyaR-mediated regulation, we used the *lacZ* reporter gene fused in-frame with the coding sequence of *yacL* and *hdeD*. β-galactosidase assays with these translational *lacZ* fusions confirmed CyaR as an efficient repressor (Supplementary Figure S5B). Unfortunately, we were not able to obtain workable translational *lacZ* fusions for *mgrB-yebO* and *nhaA-nhaR* polycistrons.

Finding additional targets of RprA sRNA

Similar to CyaR, we performed MS2-RprA affinity purification and sequenced co-purified RNAs. Ratio and reads alignment of most significant candidates are presented in Table 2 and Supplementary Figure S3, respectively.

We were able to enrich previously known targets (i.e. *rpoS* (12), *csgD* (13) and *ydaM* (13)) as well as new putative targets (i.e. *grcA, hdeD, lrhA, focA* and *tolB-pal-cpoB*). Two of
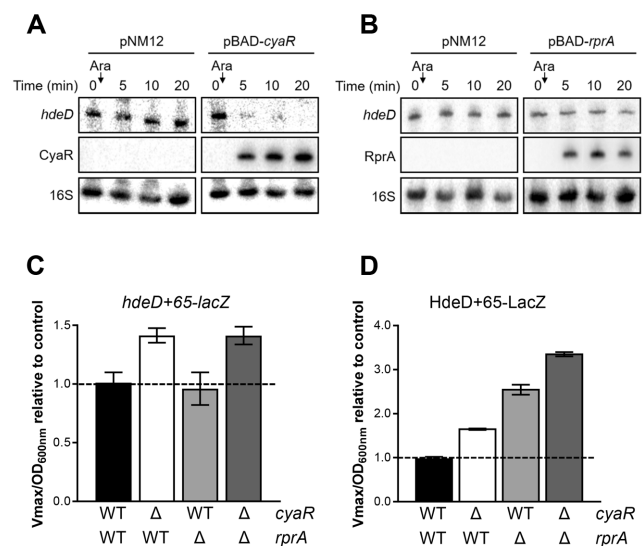
Figure 1. *hdeD* mRNA is part of two regulatory networks. Northern blot analysis of *hdeD* mRNA. The expression of (**A**) *cyaR* or (**B**) *rprA* from a pBAD promoter was induced by addition of 0.1% arabinose (Ara) when cells reached an $OD_{600\,nm}$ = 1.5 (*ΔcyaR* or *ΔrprA* background). The empty vector pNM12 was used as a control. 16S rRNA was used as a loading control. Data are representative of two independent experiments. β-galactosidase assays using (**C**) *hdeD+65-lacZ* (transcriptional) and (**D**) HdeD+65-LacZ (translational) fusions in WT (black), *ΔcyaR* (white), *ΔrprA* (gray) and *ΔcyaR ΔrprA* (dark gray) backgrounds. Samples were taken at an $OD_{600\,nm}$ of 2.0. Data represent the mean of three independent experiments ± SD.

them play a role in formate metabolism: GrcA, also called YfiD, is part of a stress-induced alternate pyruvate formate-lyase (27) and FocA is a pH-dependent formate transporter (28). As described in the Introduction, LrhA is a transcriptional factor which represses RprA sRNA synthesis. The polycistronic transcript *tolB-pal-cpoB* encodes proteins involved in outer membrane invagination during cell division (29,30).

We visualized the effect of RprA overexpression on candidate targets using northern blot assays (Supplementary Figure S6A and Figure 1B). RprA sRNA induced only a slight or no decrease of *grcA*, *hdeD* and *tolB-pal-cpoB* mRNAs signal after 20 minutes when compared to *lrhA* and the previously described target, *ydaM*. Unfortunately, no clear results were obtained for *focA* mRNA because of its weak expression in aerobic conditions. Using translational *lacZ* fusions, we noticed a clear down-regulation of all targets (35–50%), suggesting that RprA mainly regulates these targets at the translational level (Supplementary Figure S6B). The only exception was *lrhA* due to non-workable translational fusion.

hdeD mRNA, a common but differently regulated target

Regulation of hdeD *at the post-transcriptional level.* Our MAPS data pointed out that both CyaR and RprA sRNAs bind the target mRNA *hdeD* (Tables 1 and 2). We further investigated the regulatory mechanism occurring on this specific mRNA. First, we used a transcriptional *lacZ* fusion (*hdeD+65-lacZ*) to monitor the influence of each sRNA deletion on *hdeD* mRNA level in the cell (Figure 1C). While the mutation of *rprA* has no effect, the activity of *hdeD+65-lacZ* transcriptional fusion increased in absence of CyaR (1.41-fold), suggesting that CyaR induces *hdeD* mRNA decay. We also observed that β-galactosidase activities in Δ*cyaR* and Δ*cyaR* Δ*rprA* mutants are similar. This confirms the inability of RprA to induce a significant cleavage of *hdeD*, such as previous northern blot analysis (Figure 1A and B). The same results were observed when we overproduced CyaR and RprA sRNAs (Supplementary Figure S7; *hdeD+65-lacZ*).

Previously, we demonstrated that RyhB sRNA induces *sodB* mRNA degradation through a distal cleavage site (352 nt downstream from the RBS) (31). To verify the presence of a remote cleavage site on *hdeD* transcript, we used a longer *lacZ* fusion (*hdeD+602-lacZ*) containing the whole ORF of *hdeD* (except the stop codon). Again, only CyaR can significantly induce mRNA decay (Supplementary Figure S8). These data suggest that RprA strictly regulates *hdeD* mRNA at the translational level.

We then explored CyaR-dependent mRNA degradation. As RNase E is commonly involved in sRNA-mediated decay, we compared the effect of CyaR in a WT and an RNase E-thermosensitive mutant (*rne3071*) (Supplementary Figure S9A). After inactivation of RNase E at 44°C, we induced *cyaR* expression from a pBAD promoter and monitored the cellular level of *hdeD*. We noticed that, under those conditions, CyaR becomes unable to destabilize *hdeD* mRNA, which indicates that RNase E is crucial for *hdeD* degradation. The same conclusion was reached when we

used an *hdeD+65-lacZ* fusion in an *rne3071* background (Supplementary Figure S9B).

Regulation of hdeD *at the translational level.* Then, using a translational fusion (HdeD+65-LacZ), we confirmed that both CyaR and RprA induce a translational block (Figure 1D). Indeed, we noticed an increase of the β-galactosidase activity in both Δ*cyaR* and Δ*rprA* backgrounds (1.7- and 2.6-fold respectively). Notably, RprA represses *hdeD* translation more efficiently than CyaR.

Because CyaR sRNA induces mRNA decay, we performed the same experiment in an *rne3071* background to prevent degradation and focus on translation regulation (Supplementary Figure S9B). Even in absence of active degradation, CyaR repressed efficiently *hdeD* at the translational level (83%) showing that CyaR regulates *hdeD* at both the post-transcriptional and translational level.

The overproduction of CyaR or RprA also confirmed that these sRNAs repress translation of *hdeD* (Supplementary Figure S7; HdeD+65-LacZ). Remarkably, when we compared the effect of CyaR overexpression in Δ*cyaR* and Δ*cyaR* Δ*rprA* mutants, we noticed an increase of the post-transcriptional repression in absence of RprA (1.4-fold for *hdeD+65* and 1.1-fold for HdeD+65) (Supplementary Figure S7). We observed the same result for RprA in absence of CyaR, but at the translational level (1.5-fold for HdeD+65). As a result, it seems that CyaR activity is hindered by the presence of RprA, and vice-versa. We can assume that CyaR and RprA share a common binding site on *hdeD* mRNA or at least that these binding sites overlap.

Both CyaR and RprA sRNAs bind to the 5′-UTR of *hdeD* mRNA

To identify both CyaR and RprA sRNAs binding sites on the *hdeD* sequence, we performed lead acetate (PbAc) probing assays using a 5′-radiolabeled *hdeD+195* RNA fragment incubated with CyaR or RprA (Figure 2A). In the presence of CyaR, we observed a clear protection of nucleotides +26 to +35 containing the Shine-Dalgarno sequence (SD). In the case of RprA, an uncommon binding site is noticed, from +1 to +11 nucleotides. In silico predictions by IntaRNA software (32) suggest the same pairing sites on *hdeD* mRNA. Binding sites are represented in Figure 2B. Remarkably, an additional but slight protection is observed in the RBS. To verify this, we used *in line* probing assays in presence or absence of RprA (Figure 2C). In addition to the first protected region in the 5′end of *hdeD*, we noticed a second site from nucleotides +26 to +38, covering the SD and start codon of *hdeD* (Figure 2D). Interestingly, the same region of RprA (seed sequence) is used to base-pair with both putative pairing sites, suggesting that two RprA molecules could bind to the 5′-UTR of *hdeD*.

Repression of *hdeD* translation requires the binding of two RprA molecules

Our *in vitro* probing assays (Figure 2) suggested the presence of two putative RprA binding sites on *hdeD*. We hypothesized that RprA could target both the 5′end and the RBS of *hdeD* mRNA. To validate this, we individually mutated both potential binding sites as indicated in Figure 3A
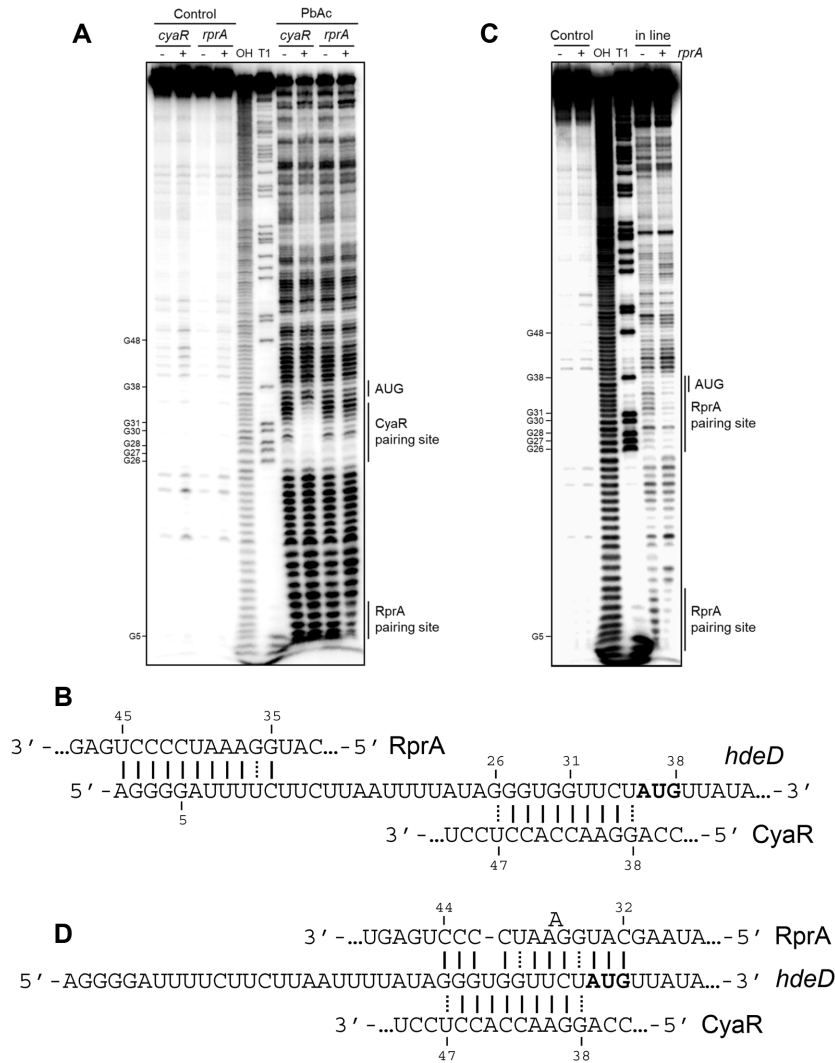
Figure 2. The 5′-UTR of *hdeD* mRNA is targeted by both CyaR and RprA *in vitro*. (**A**) Lead acetate (PbAC) probing of 5′end-radiolabeled *hdeD*+195 incubated in presence or absence of CyaR and RprA. OH, alkaline ladder; T1, RNase T1 ladder. The numbers to the left indicate sequence positions with respect to the +1 of *hdeD*. (**B**) Validated pairing between *hdeD* and both sRNAs. (**C**) In-line (MgCl₂) probing of 5′end-radiolabeled *hdeD*+195 in presence or absence of RprA. Samples were incubated with MgCl₂ during 48 h. OH, alkaline ladder; T1, RNase T1 ladder. (**D**) Representation of the second validated pairing site of RprA on *hdeD* mRNA.

(5′mut and RBSmut). The effect of each mutation on the absolute β-galactosidase activity of HdeD+65-LacZ fusion is shown in Supplementary Figure S10. Even if the mutation of the spacer sequence between the SD and the initiator codon strongly reduces β-galactosidase activity, we were able to obtain a workable *lacZ* fusion.

We performed β-galactosidase assays using HdeD+65–5′mut-LacZ (Figure 3B) and HdeD+65-RBSmut-LacZ (Figure 3C) translational fusions. In Figure 3B, we showed that the 5′end mutation of *hdeD* fully negates RprA repression, but not CyaR repression. This confirms that the 5′end of *hdeD* is essential for RprA activity. The second pairing site located in the RBS is also crucial, as suggested by the complete loss of RprA effect on HdeD+65-RBSmut-LacZ (Figure 3C).

To prove a direct pairing between RprA and *hdeD* mRNA, we used compensatory mutations for each de-

scribed mutant (Supplementary Figure S11). First, we confirmed that RprA failed to down-regulate HdeD+65–5′mut-LacZ translational fusion (Supplementary Figure S11A). Second, the same effect is observed by mutating the corresponding binding site on RprA (RprA-5′mut) with an HdeD+65-LacZ construct. Finally, overexpression of RprA compensatory mutant re-establishes RprA-mediated regulation of HdeD+65–5′mut. Hence, RprA directly binds to the 5′end of *hdeD* mRNA.

We then performed the same experiment with the second pairing site (RBSmut) (Supplementary Figure S11B). We noticed a strong loss of regulation by mutating either *hdeD* or RprA. However, we still observed a significant RprA-mediated regulation with HdeD+65-RBSmut (30% instead of 60% for the WT construct). Here, we preserved the SD sequence and only mutated the adjacent nucleotides. It seems that the binding site is partially disrupted but still provides
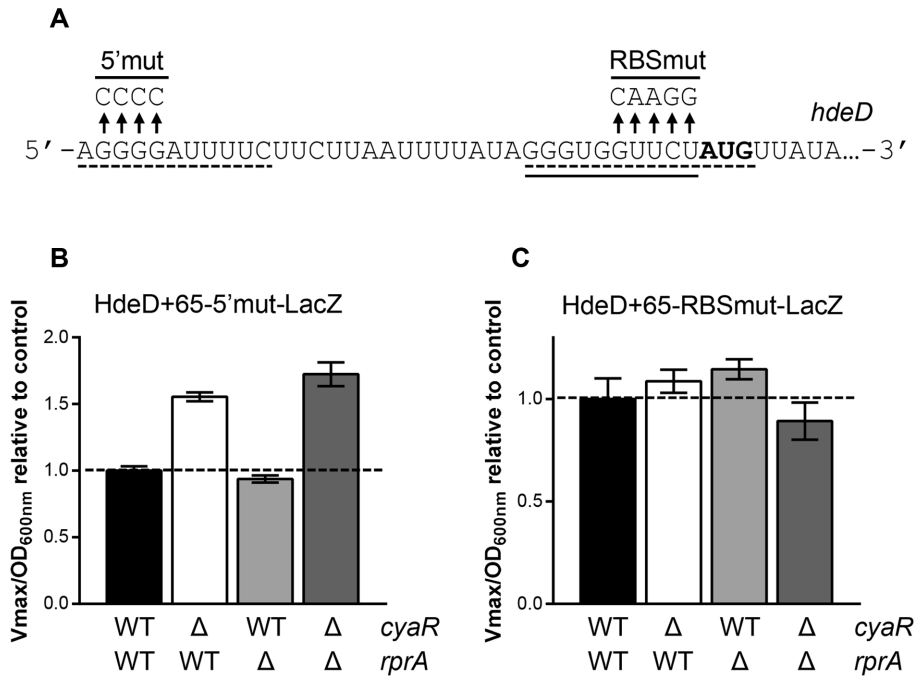
Figure 3. Two RprA binding sites are essential for *hdeD* regulation *in vivo*. (**A**) Mutation of the 5′end (5′mut) and RBS (RBSmut) of *hdeD* mRNA. Solid line and dashed lines indicate CyaR and RprA binding sites, respectively. The translation start codon is shown in bold. β-galactosidase assays using (**B**) HdeD+65–5′mut-LacZ and (**C**) HdeD+65-RBSmut-LacZ translational fusions in WT (black), Δ*cyaR* (white), Δ*rprA* (gray) and Δ*cyaR* Δ*rprA* (dark gray) backgrounds. Samples were taken at an $OD_{600 nm}$ of 2.0. Data represent the mean of three independent experiments ± SD.

enough complementarities, explaining the residual activity of RprA. Unfortunately, we were not able to restore the regulation using compensatory mutants (Supplementary Figure S11B). Nonetheless, accumulated results strongly argue that RprA regulates *hdeD* through dual binding of 5′ and RBS sites.

**Hfq binding to the 5′-UTR of *hdeD* is necessary to induce mRNA decay**

Using the HdeD+65-RBSmut-LacZ translational fusion (Figure 3A), we observed that the sequence between the SD sequence and the start codon is essential for CyaR-mediated regulation of *hdeD* mRNA (Figure 3C). As observed for RprA, the mutation of either *hdeD* or CyaR led to a significant derepression (Supplementary Figure S12). Again, we were not able to restore CyaR activity using compensatory mutations. However, evidence tends to validate a direct binding of CyaR to the RBS of *hdeD*.

Although CyaR and RprA sRNAs bind to the RBS sequence of *hdeD* mRNA, only CyaR induces a strong and rapid mRNA decay (Figure 1A, Supplementary Figures S5A and S6A). Data presented in Supplementary Figure S9 strongly suggest that RNase E is actively recruited to induce the degradation of *hdeD* mRNA. Interestingly, we noticed the presence of two A/U-rich motif, upstream of the CyaR binding site (nucleotides +15 to +25) and just after the initiator codon (nucleotides +39 to +47) (Figure 4A). Both Hfq and RNase E are known to preferentially bind to this motif (33,34).

To determine if the A/U rich sequence localized close to the AUG codon (nucleotides +39 to +47) is involved

in *hdeD* decay, we removed it using a shorter *lacZ* fusion (*hdeD*+40-*lacZ*; Figure 4B). We previously used this approach to determine the RNAse E cleavage site on *sodB* (31), *sdhC* (35) and *rbsD* (17). Even if *cyaR* was overexpressed, no regulation at the post-transcriptional level was observed, hinting that the RNase E cleavage site is localized between nucleotides +40 and +65. As a control, we showed that CyaR is still able to pair with *hdeD* mRNA and block its translation (HdeD+40-LacZ; 73%).

Then, we monitored the effect of the mutation of the second A/U-rich sequence (MH4), localized upstream of CyaR binding site (Figure 4A). We verified that MH4 mutation does not affect the basal β-galactosidase activity of HdeD+65-LacZ fusion (Supplementary Figure S10). Using *hdeD*+65-MH4-*lacZ* transcriptional fusion, we observed a complete loss of regulation by CyaR (Figure 4C). Remarkably, the mutation MH4 does not prevent translational repression by CyaR as shown by HdeD+65-MH4-LacZ translational fusion (Figure 4C). In 2015, Schu *et al.* (34) have shown that target mRNAs regulated by Class II sR-NAs (such as CyaR) contain an A/U-rich sequence allowing the binding of the RNA chaperone protein Hfq. We first validated that Hfq recognizes and binds this A/U-rich motif in the 5′-UTR of *hdeD* using *in vitro* probing (Supplementary Figure S13). The identified binding site is indicated in Figure 4A. Then, we performed β-galactosidase assays in a Δ*hfq* background (Figure 4D). CyaR overexpression has no effect on an *hdeD*+65-*lacZ* transcriptional fusion, suggesting that Hfq is involved in *hdeD* mRNA decay. However, CyaR is described as an Hfq-dependent sRNA, notably for its stability (7,8). Thus, results obtained in Figure 4D could
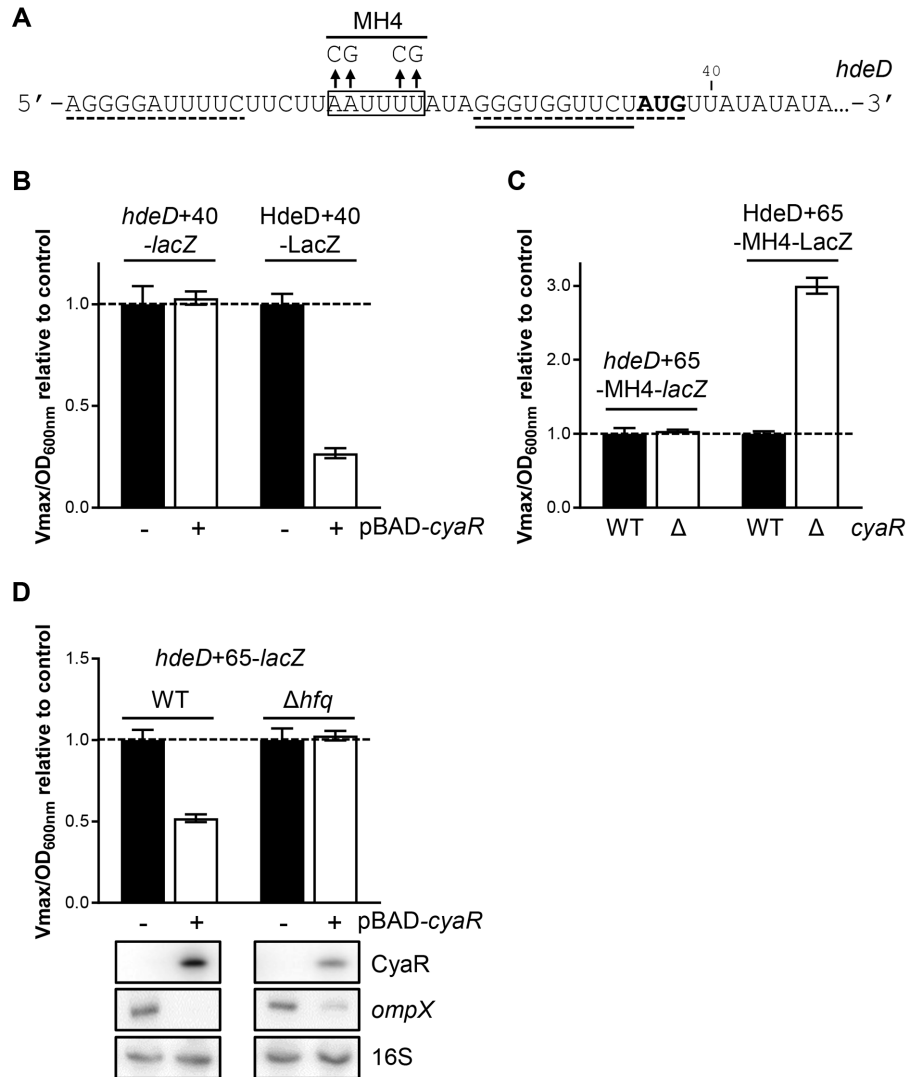
Figure 4. Hfq binding to *hdeD* mRNA is required to induce mRNA decay. (**A**) Mutation of the A/U-rich region (MH4) localized between CyaR and RprA binding sites. Boxed text corresponds to the *in vitro* determined Hfq binding site. Solid line and dashed lines indicate CyaR and RprA binding sites, respectively. The translation start codon is shown in bold. (**B**) β-Galactosidase assays using *hdeD*+40-*lacZ* transcriptional fusion or HdeD+40-LacZ translational fusion in a Δ*cyaR* background. Strains carry either an empty vector (pNM12; black) or a pBAD-*cyaR* (white). The expression of *cyaR* was induced by addition of 0.1% arabinose when cells reached an $OD_{600 nm} = 0.5$. Samples were taken at an $OD_{600 nm}$ of 1.8. Data represent the mean of three independent experiments ± SD. (**C**) β-Galactosidase assays using *hdeD*+65-MH4-*lacZ* transcriptional fusion or HdeD+65-MH4-LacZ translational fusion in WT (black) and Δ*cyaR* (white) backgrounds. Samples were taken at an $OD_{600 nm}$ of 2.0. (**D**) β-Galactosidase assays using *hdeD*+65-*lacZ* transcriptional fusions in Δ*cyaR* Δ*rprA* and Δ*cyaR* Δ*rprA* Δ*hfq* backgrounds. Strains carry either an empty vector (pNM12; black) or a pBAD-*cyaR* (white). Samples were taken 2h after the induction of *cyaR* expression with 0.1% arabinose (at $OD_{600 nm}$ of 0.5). Northern blot assays were performed at the same time to monitor the level of CyaR sRNA and *ompX* mRNA. 16S rRNA was used as a loading control. Data are representative of two independent experiments.

be also explained by the lack of stability or functionality of CyaR sRNA in a Δ*hfq* background. To discard this hypothesis, we extracted total RNA of samples used in Figure 4D and observed a significant amount of CyaR after 2h. Moreover, we demonstrated that CyaR is still functional as CyaR induces the decay of *ompX* mRNA (61% in Δ*hfq* strain compared to 88% in WT). Therefore, the binding of Hfq to the 5′-UTR of *hdeD* mRNA is critical to induce its decay.

Interchanging the seed region of sRNAs also interchanges the ability to degrade *hdeD* mRNA

To determine if the signal required to induce the degradation of *hdeD* mRNA is held in the pairing region of CyaR, we decided to switch seed regions of CyaR and RprA. As both sequences are part of a stem-loop structure, we simply exchanged them (CyaR-seed* and RprA-seed*; see Figure 5A). As shown in Figure 5B, the modified version of CyaR sRNA (carrying RprA seed) has lost the ability to induce *hdeD* mRNA decay (4% instead of 45% for WT CyaR). As a control, we verified that CyaR-seed* construct is stable *in vivo* using northern blot analysis (Figure 5B). Moreover,
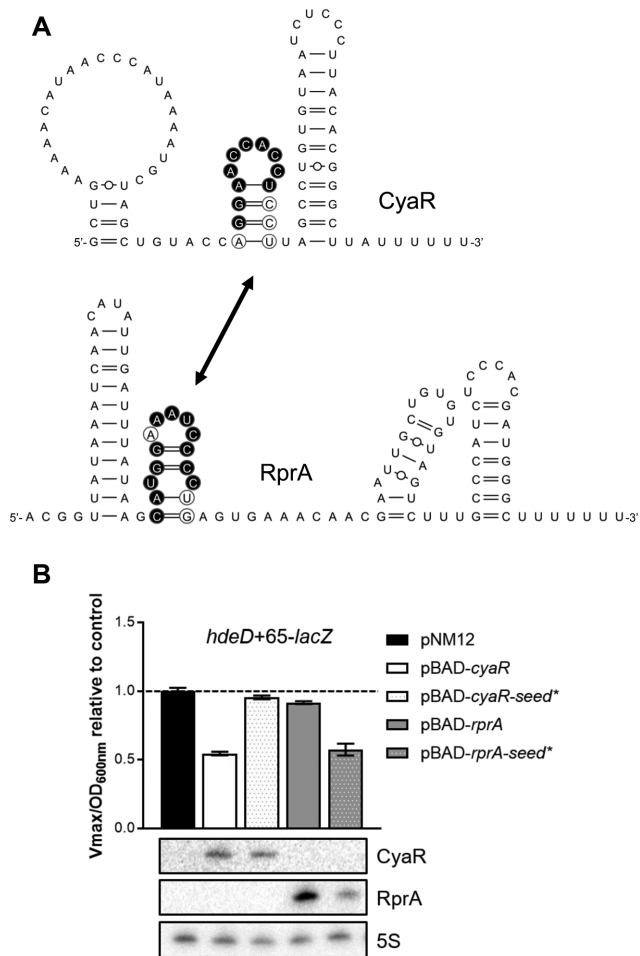
Figure 5. Interchanging the seed sequence of CyaR and RprA also interchanges the ability to induce *hdeD* mRNA decay. (**A**) Secondary structures of CyaR and RprA sRNAs determined using Mfold software (35) and visualized with VARNA software (36). To construct CyaR-seed* and RprA-seed*, the hairpins bearing the seed region of CyaR and RprA were switched. Exchanged nucleotides are circled. Binding sites are indicated in black. (**B**) β-Galactosidase assays with *hdeD*+65 transcriptional *lacZ* fusion in a Δ*cyaR* Δ*rprA* background. Overexpression of *cyaR, cyaR-seed**, *rprA* or *rprA-seed** was induced by addition of 0.1% arabinose when cells reached an $OD_{600\,nm}$ of 0.5. Samples were taken at an $OD_{600\,nm}$ = 1.5. Data represent the mean of three independent experiments ± SD.

we observed that CyaR-seed* is still able to block the initiation of *hdeD* translation (Supplementary Figure S14). On the contrary, RprA-seed* construct (RprA carrying CyaR binding sequence) is now able to promote *hdeD* degradation (43% compared to 45% for WT CyaR). Thus, the seed region of CyaR is sufficient to induce *hdeD* mRNA decay, even within a sRNA known to be ineffective to degrade this target.

CyaR-dependent regulation of *hdeD* mRNA is hindered in presence of glucose or sodium pyruvate

As described in Supplementary Figure S15, CyaR and RprA sRNAs are under the control of major transcriptional regulators, responding to specific stimuli. Notably, *cyaR* expression is repressed in presence of glucose (CRP-AMPc

and CpxR) and pyruvate (CpxR) (7,38). Consequently, these growth conditions may favor the RprA-mediated regulation of *hdeD* mRNA. To validate this assumption, we monitored the β-galactosidase activity of an HdeD+65-LacZ translational fusion in presence of 0.4% glucose (Figure 6A) or 0.8% sodium pyruvate (Figure 6B). This led to the complete inhibition of CyaR synthesis as no difference was observed between WT and Δ*cyaR* strains. The same result is noticed when we compared the Δ*rprA* and Δ*cyaR* Δ*rprA* backgrounds. However, RprA still negatively regulates *hdeD* mRNA at the translational level.

To confirm that the repression of CyaR activity in presence of glucose or pyruvate is notably due to the response regulator CpxR, we performed similar experiments in a Δ*cpxR* background (Figure 6C). In absence of CyaR, we observed a comparable derepression of HdeD+65-LacZ fusion when we compared *cpxR*[+] (Figure 1D; 1.41-fold) and Δ*cpxR* backgrounds (Figure 6C; 1.37-fold). As in Figure 6A, the mutation of *cyaR* had no effect in presence of 0.4% glucose, certainly due to the inactivation of the cAMP-CRP system. On the contrary, CyaR sRNA still negatively regulates HdeD+65-LacZ fusion in presence of 0.8% sodium pyruvate (Figure 6C; 1.40-fold). This confirms that CpxR blocks *cyaR* transcription in response to pyruvate. Thus, depending on specific growth conditions, RprA-dependent regulation will be favored over that of CyaR and vice versa.

DISCUSSION

In this study, we demonstrated that both CyaR and RprA can block the translation initiation of *hdeD* but only CyaR induces mRNA decay. In bacteria, the sRNA-dependent translation repression is generally coupled with passive or active degradation of targeted mRNA (6). Upon translational inhibition, 'naked' mRNA becomes more sensitive to RNase E nucleolytic attacks (passive degradation). To speed up the process, sRNAs can actively recruit RNase E via the formation of a sRNA/Hfq/RNase E complex (active degradation), where Hfq directly binds the C-terminal region of RNase E (39). However, the mechanism of recruitment of RNase E is only partially understood. Our results indicated that both Hfq and RNase E are required for CyaR-dependent *hdeD* mRNA decay. Here, the role of Hfq is not limited to facilitating CyaR:*hdeD* interaction or stabilizing CyaR sRNA. Although nothing prevents the formation of the CyaR/Hfq/RNase E complex, our model suggests that Hfq should first recognize an A/U-rich motif in the 5′-UTR of *hdeD*. Therefore, a direct contact between Hfq and *hdeD* mRNA is essential to actively induce *hdeD* mRNA decay via RNase E (Figure 7).

According to Schu *et al.* (34), sRNAs could be classified in function of their interaction with Hfq. Basically, an Hfq hexamer carries three RNA-binding elements: a proximal face, a rim and a distal face. Whereas class I sRNAs bind to Hfq proximal face and rim, class II sRNAs prefer its proximal and distal faces. The remaining binding surface interacts with the targeted mRNA. Each Hfq face recognizes a specific sequence: U-rich sequence for the proximal face, ARN motif for the distal face and A/U-rich sequence for the rim. CyaR is depicted as a class II sRNA and *hdeD* bears an A/U-rich sequence which is optimal for the for-
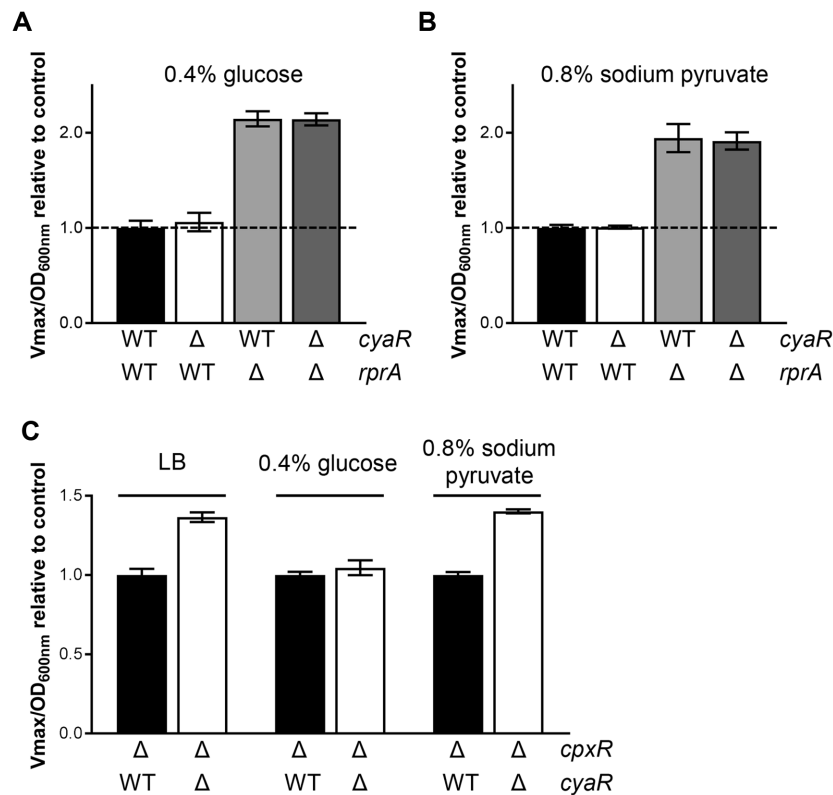
Figure 6. CyaR-dependent regulation of *hdeD* mRNA is hindered in presence of glucose or sodium pyruvate. β-galactosidase assays using HdeD+65-LacZ (translational) fusions in WT (black), Δ*cyaR* (white), Δ*rprA* (gray) and Δ*cyaR* Δ*rprA* (dark gray) backgrounds. When cells reached an OD$_{600 \text{ nm}}$ = 0.5, (**A**) 0.4% glucose or (**B**) 0.8% sodium pyruvate was added. (**C**) β-Galactosidase assays using HdeD+65-LacZ (translational) fusions in Δ*cpxR* (black) and Δ*cpxR* Δ*cyaR* (white) in LB medium supplemented with 0.4% glucose or 0.8% sodium pyruvate. LB medium is used as a control. Samples were taken at an OD$_{600 \text{ nm}}$ of 2.0. Data represent the mean of three independent experiments ± SD.

mation of CyaR/*hdeD*/Hfq complex. Note that this supports a model where only one Hfq hexamer is required to bind simultaneously CyaR and *hdeD*. Interestingly, RprA is a non-exclusive class II sRNA (34), suggesting that Hfq should bind *hdeD* mRNA with its rim face as well.

Remarkably, by interchanging seed sequences of CyaR and RprA, we also interchanged the outcome at the posttranscriptional level. We previously used this approach with RyhB and Spot42 sRNAs (35). Both sRNAs were characterized as negative regulators of *sdhC* mRNA. While RyhB classically pairs with the SD sequence, Spot42 binds far upstream and must recruit Hfq close to the RBS to compete with initiating ribosomes. These distinct mechanisms of action were also interchanged by switching respective seed regions. Similarly, we confirmed that all the signal required to induce *hdeD* mRNA decay is contained in the short seed region of CyaR. In terms of similarities, both seeds encompass a short stem-loop structure located at nucleotides 36 and 31 from the 5′end of CyaR and RprA, respectively. As indicated in Figure 2D, CyaR base-pairs with *hdeD* mRNA via a short and perfect sequence (energy –8.84 kcal/mol, determined by IntaRNA (32)), while RprA binding site bears two non-interacting nucleotides (energy –7.71 kcal/mol) and is longer, overlapping the AUG initiator codon. However, the role of each single nucleotide constituting the seed sequence is still poorly understood (e.g. in mRNA target selection or in sRNA-mediated regulatory mechanism). In-

terestingly, recent studies have assessed the importance of single nucleotide changes, notably in the sRNA seed region (40–41). They determined that: (a) as little as one single nucleotide mutation can annihilate sRNA-dependent regulation, and (b) not all nucleotides of the seed are critical (nonessential bases). To complicate matters further, critical nucleotides can change in function of the targeted mRNA. As a conclusion, slight nucleotide substitutions could be accountable for the difference between CyaR and RprA regulatory mechanisms. Further work will be required to validate this assumption.

It is even more difficult to draw conclusions from seed characteristics as RprA is one of the rare examples of sRNAs that does not trigger mRNA decay upon binding. Indeed, only a few sRNAs were suggested to act primarily at the translational level in bacteria (42–44). This phenomenon seems target specific because RprA can induce the rapid degradation of other targets (i.e. *csgD*, *ydaM* and *lrhA* transcripts) (Supplementary Figure S6A and Table S4). Nevertheless, it remains difficult to compare those examples to highlight determinants or factors required to seal the fate of targeted mRNAs. Indeed, nothing is known about *ydaM* and *lrhA* decay. Moreover, RNase E has only a limited effect on *csgD* stability (13).

Consistent with the classical model of sRNA-dependent translational repression, the binding of a sRNA to the RBS is sufficient to interfere with ribosome assembly and con-
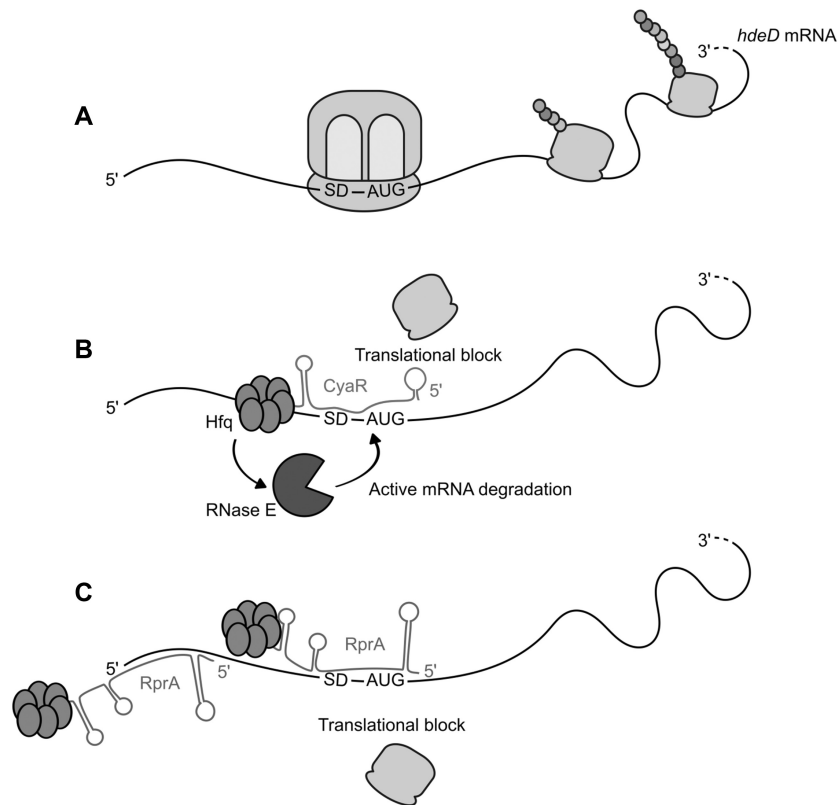
Figure 7. Descriptive model for CyaR and RprA-mediated *hdeD* regulation. (**A**) Under non-inducing conditions, *hdeD* mRNA is normally translated. Depending on environmental stimuli, CyaR and/or RprA are expressed within the cell, resulting in two distinct outcomes. (**B**) CyaR binds to the RBS of *hdeD* and interferes with translation initiation. In addition, CyaR induces an active degradation of *hdeD* mRNA. For this purpose, Hfq protein has to recognize and bind to both CyaR and the 5′-UTR of *hdeD* (A/U-rich motif). Through a direct protein:protein interaction, Hfq potentially recruits RNase E resulting in an active RNase E-dependent *hdeD* decay. (**C**) Two molecules of RprA are required to suppress *hdeD* translation. Indeed, RprA binds to two different sites, which are both essential for translational block. RprA has no effect on *hdeD* stability. The secondary structure of CyaR and RprA sRNAs was predicted in silico (Figure 5).

sequently translation initiation. Although both CyaR and RprA target the RBS of *hdeD*, only CyaR meets the criteria to directly block translation without any additional requirements. The RprA-mediated mechanism of *hdeD* regulation remains unclear, but is quite uncommon (Figure 7). Indeed, we demonstrated that mutation of either site I (5′end) or site II (RBS) completely abolished RprA effect on *hdeD* translation (Figure 3). This differs from previously known examples where both binding sites act additively. For instance, two regions of base-pairing were identified on *csgD* mRNA, another target of RprA (13). Site I (close to the 5′end) and site II (RBS) seem functionally redundant as the mutation of both sites is required to affect RprA-mediated regulation of *csgD* mRNA. Binding two sites in the 5′UTR of a specific target as shown here for RprA is not a unique feature. For example, Bos *et al.* also suggested an additive effect of RyhB pairing with two distinct sites in the 5′-UTR of *msrB* mRNA (45). Interestingly, the second base-pairing site can be localized in the coding sequence (CDS) instead of in the 5′end. For example, SgrS base-pairs twice on *asd* mRNA (46). Each individual site is sufficient for translational regulation but pairing at both sites is required for optimal *asd* repression. Similarly, both MicF sRNA pairing sites on *lpxR* mRNA act additively in *Salmonella* Typhimurium, the sec-

ond binding site (CDS) being essential to induce RNase E cleavage (47).

CyaR and RprA are under the control of multiple regulatory systems (i.e. sigma factors, two-component systems), which themselves respond to numerous and various stimuli (Supplementary Figure S15). Depending on stimuli detected by cells, one of these regulators will prevail, resulting in one of the situations presented in Figure 7. A perfect example is the CpxAR two-component system which has an antagonistic effect on CyaR and RprA. In presence of a preferred source of carbon (e.g. pyruvate), the response regulator CpxR is phosphorylated (38) and, therefore, CyaR synthesis is shut down. Inversely, CyaR should take over in presence of a non-preferred source of carbon and induce total degradation of *hdeD* mRNA. Since RprA and CyaR are both produced in stationary phase of growth, they could potentially compete for binding. However, we only observed a competition when CyaR or RprA were overexpressed (Supplementary Figure S7), suggesting that *hdeD* mRNA is not limiting in endogenous conditions (Figure 1D and Supplementary Figure S16).

Other sRNAs belong to the Cpx regulon. For instance, Chao and Vogel (48) demonstrated that CpxR directly triggers the transcription of *cpxP* gene. Afterward, the 3′UTR of *cpxP* mRNA is processed by RNase E leading to the

release of CpxQ sRNA. Interestingly, both CpxP protein and CpxQ sRNA are involved in the inner membrane homeostasis. MicF, OmrA and OmrB sRNAs, three post-transcriptional regulators of outer membrane proteins, are also regulated by the response regulator CpxR, although indirectly (3,49). Through the induction of *mzrA* gene, CpxR indirectly activates the histidine kinase EnvZ, which is part of the EnvZ/OmpR two-component system (3). Indeed, MzrA protein is known to interact with EnvZ and to activate it. Then, EnvZ phosphorylates OmpR, enabling the transcription of *micF*, *omrA* and *omrB* genes (3,49). However, there is no evidence supporting the involvement of aforementioned sRNAs in *hdeD* mRNA regulation.

According to Mates *et al.*, HdeD is involved in an acid-resistance mechanism exhibited only at high cellular density (25). As described in Supplementary Figure S16, *hdeD* mRNA is most exclusively expressed during the stationary phase of growth, which is consistent with a role of HdeD protein at high density (>2 of $OD_{600\,nm}$). Notably, *hdeD* gene is part of an acid fitness island and its expression is directly activated by GadX and GadE (also named YhiE), two regulators of the acid resistance system (25,50). Nonetheless, its role remains poorly understood. Indeed, studies failed to reach a consensus: the effect of HdeD depletion seems to vary upon the methodology used to test acid resistance (51,52).

The function of other putative targets of CyaR and RprA is also related to pH homeostasis (Supplementary Figure S15). Both GrcA and FocA reduce the accumulation of acidic metabolites within the cell, in a pH-dependent manner (28,53). MgrB influences the expression of multiple acid stress-associated genes by sequestering the histidine kinase of the PhoQP two-component system (24). On the contrary, the Na+:H+ antiporter NhaA and, by extent, its regulator NhaR are involved in alkaline pH homeostasis (54).

In *E. coli*, most 5′UTRs are between 20 and 40 nucleotides long (55). Within the 35 nt-long *hdeD* 5′-UTR, we discovered three sRNA binding sites as well as one Hfq recognition motif (Figure 4A). Other mRNAs such as *rpoS* and *csgD* are major hubs for signal integration. Both *rpoS* and *csgD* mRNAs bear relatively large 5′-UTR, around 570 and 140 nt respectively. The 5′-UTR of *rpoS* mRNA is the 'runway' for four sRNAs (DsrA, RprA, ArcZ and OxyS) and Hfq (56,57) and at least six sRNAs were shown to fine-tune CsgD translation (58,59). Our data suggest that a huge 5′-UTR is not required to integrate multiple signals.

The last decade has been characterized by conceptual and technical innovations enabling the development of high-throughput RNA sequencing methods with the aim of unraveling all sRNA:RNA interactions (60). These are based on RNA co-purification with either a specific protein (61–63) or a particular sRNA (65,66). For instance, MAPS technology, based on the use of MS2-tagged sRNA, has already demonstrated its efficiency by revealing RyhB, RybB and DsrA sRNA regulatory networks (17,18). In the current study, we explored two additional regulatory networks which are under the control of CyaR and RprA sRNAs. Recently, Melamed *et al.* (63) developed a new method called RIL-Seq (for RNA interaction by ligation and sequencing), based on the co-purification of sRNA:RNA complexes associated with the Hfq-tagged protein. RIL-

Seq and MAPS were performed in similar conditions (LB medium, exponential and stationary phases). The putative CyaR-regulated mRNAs identified by MAPS were also revealed by RIL-Seq (among 313 potential CyaR:RNA interactions). However, only two of those transcripts were highly co-purified by RIL-Seq, *mgrB-yebO* and *nhaA-nhaR*. Surprisingly, *hdeD* and *grcA*, two strongly enriched mRNAs with MAPS, were not identified by RIL-Seq as potentially regulated by RprA. Conversely, MAPS failed to significantly capture top putative targets determined by RIL-Seq. Therefore, the information gained through distinct co-purification approaches seems not redundant but complementary.

AVAILABILITY

MAPS data have been deposited in GEO under accession GSE90128 (MS2-CyaR) and GSE80020 (MS2-RprA).

SUPPLEMENTARY DATA

Supplementary Data are available at NAR Online.

FUNDING

REFERENCES

1. Jung,K., Fried,L., Behr,S. and Heermann,R. (2012) Histidine kinases and response regulators in networks. *Curr. Opin. Microbiol.*, **15**, 118–124.
2. Ortet,P., Whitworth,D.E., Santaella,C., Achouak,W. and Barakat,M. (2015) P2CS: updates of the prokaryotic two-component systems database. *Nucleic Acids Res.*, **43**, D536–D541.
3. Vogt,S.L., Evans,A.D., Guest,R.L. and Raivio,T.L. (2014) The Cpx envelope stress response regulates and is regulated by small noncoding RNAs. *J. Bacteriol.*, **196**, 4229–4238.
4. Grabowicz,M. and Silhavy,T.J. (2017) Envelope stress responses: an interconnected safety net. *Trends Biochem. Sci.*, **42**, 232–242.
5. Wagner,E.G. and Romby,P. (2015) Small RNAs in bacteria and archaea: who they are, what they do, and how they do it. *Adv. Genet.*, **90**, 133–208.
6. Lalaouna,D., Simoneau-Roy,M., Lafontaine,D. and Masse,E. (2013) Regulatory RNAs and target mRNA decay in prokaryotes. *Biochim. Biophys. Acta*, **1829**, 742–747.
7. Johansen,J., Eriksen,M., Kallipolitis,B. and Valentin-Hansen,P. (2008) Down-regulation of outer membrane proteins by noncoding RNAs: unraveling the cAMP-CRP- and sigmaE-dependent CyaR-ompX regulatory case. *J. Mol. Biol.*, **383**, 1–9.
8. Papenfort,K., Pfeiffer,V., Lucchini,S., Sonawane,A., Hinton,J.C. and Vogel,J. (2008) Systematic deletion of Salmonella small RNA genes identifies CyaR, a conserved CRP-dependent riboregulator of OmpX synthesis. *Mol. Microbiol.*, **68**, 890–906.
9. De Lay,N. and Gottesman,S. (2009) The Crp-activated small noncoding regulatory RNA CyaR (RyeE) links nutritional status to group behavior. *J. Bacteriol.*, **191**, 461–476.
10. Wright,P.R., Richter,A.S., Papenfort,K., Mann,M., Vogel,J., Hess,W.R., Backofen,R. and Georg,J. (2013) Comparative genomics boosts target prediction for bacterial small RNAs. *Proc. Natl. Acad. Sci. U.S.A.*, **110**, E3487–E3496.
11. Bruckner,R. and Titgemeyer,F. (2002) Carbon catabolite repression in bacteria: choice of the carbon source and autoregulatory limitation of sugar utilization. *FEMS Microbiol. Lett.*, **209**, 141–148.
12. Majdalani,N., Chen,S., Murrow,J., St John,K. and Gottesman,S. (2001) Regulation of RpoS by a novel small RNA: the characterization of RprA. *Mol. Microbiol.*, **39**, 1382–1394.

13. Mika,F., Busse,S., Possling,A., Berkholz,J., Tschowri,N., Sommerfeldt,N., Pruteanu,M. and Hengge,R. (2012) Targeting of csgD by the small regulatory RNA RprA links stationary phase, biofilm formation and cell envelope stress in Escherichia coli. *Mol. Microbiol.*, **84**, 51–65.

14. Papenfort,K., Espinosa,E., Casadesus,J. and Vogel,J. (2015) Small RNA-based feedforward loop with AND-gate logic regulates extrachromosomal DNA transfer in Salmonella. *Proc. Natl. Acad. Sci. U.S.A.*, **112**, E4772–E4781.

15. Majdalani,N., Hernandez,D. and Gottesman,S. (2002) Regulation and mode of action of the second small RNA activator of RpoS translation, RprA. *Mol. Microbiol.*, **46**, 813–826.

16. Peterson,C.N., Carabetta,V.J., Chowdhury,T. and Silhavy,T.J. (2006) LrhA regulates rpoS translation in response to the Rcs phosphorelay system in Escherichia coli. *J. Bacteriol.*, **188**, 3175–3181.

17. Lalaouna,D., Morissette,A., Carrier,M.C. and Masse,E. (2015) DsrA regulatory RNA represses both hns and rbsD mRNAs through distinct mechanisms in Escherichia coli. *Mol. Microbiol.*, **98**, 357–369.

18. Lalaouna,D., Carrier,M.C., Semsey,S., Brouard,J.S., Wang,J., Wade,J.T. and Masse,E. (2015) A 3′ external transcribed spacer in a tRNA transcript acts as a sponge for small RNAs to prevent transcriptional noise. *Mol. Cell*, **58**, 393–405.

19. Aiba,H., Adhya,S. and de Crombrugghe,B. (1981) Evidence for two functional gal promoters in intact Escherichia coli cells. *J. Biol. Chem.*, **256**, 11905–11910.

20. Church,G.M. and Gilbert,W. (1984) Genomic sequencing. *Proc. Natl. Acad. Sci. U.S.A.*, **81**, 1991–1995.

21. Lalaouna,D., Prevost,K., Eyraud,A. and Masse,E. (2017) Identification of unknown RNA partners using MAPS. *Methods*, **117**, 28–34.

22. Schneider,K.L., Pollard,K.S., Baertsch,R., Pohl,A. and Lowe,T.M. (2006) The UCSC archaeal genome browser. *Nucleic Acids Res.*, **34**, D407–D410.

23. Majdalani,N., Cunning,C., Sledjeski,D., Elliott,T. and Gottesman,S. (1998) DsrA RNA regulates translation of RpoS message by an anti-antisense mechanism, independent of its action as an antisilencer of transcription. *Proc. Natl. Acad. Sci. U.S.A.*, **95**, 12462–12467.

24. Lippa,A.M. and Goulian,M. (2009) Feedback inhibition in the PhoQ/PhoP signaling system by a membrane peptide. *PLoS Genet.*, **5**, e1000788.

25. Mates,A.K., Sayed,A.K. and Foster,J.W. (2007) Products of the Escherichia coli acid fitness island attenuate metabolite stress at extremely low pH and mediate a cell density-dependent acid resistance. *J. Bacteriol.*, **189**, 2759–2768.

26. Dover,N., Higgins,C.F., Carmel,O., Rimon,A., Pinner,E. and Padan,E. (1996) Na+-induced transcription of nhaA, which encodes an Na+/H+ antiporter in Escherichia coli, is positively regulated by nhaR and affected by hns. *J. Bacteriol.*, **178**, 6508–6517.

27. Zhu,J., Shalel-Levanon,S., Bennett,G. and San,K.Y. (2007) The YfiD protein contributes to the pyruvate formate-lyase flux in an Escherichia coli arcA mutant strain. *Biotechnol. Bioeng.*, **97**, 138–143.

28. Sawers,R.G. (2005) Formate and its role in hydrogen production in Escherichia coli. *Biochem. Soc. Trans.*, **33**, 42–46.

29. Gray,A.N., Egan,A.J., Van't Veer,I.L., Verheul,J., Colavin,A., Koumoutsi,A., Biboy,J., Altelaar,A.F., Damen,M.J., Huang,K.C. et al. (2015) Coordination of peptidoglycan synthesis and outer membrane constriction during Escherichia coli cell division. *eLife*, **4**.

30. Gerding,M.A., Ogata,Y., Pecora,N.D., Niki,H. and de Boer,P.A. (2007) The trans-envelope Tol-Pal complex is part of the cell division machinery and required for proper outer-membrane invagination during cell constriction in E. coli. *Mol. Microbiol.*, **63**, 1008–1025.

31. Prevost,K., Desnoyers,G., Jacques,J.F., Lavoie,F. and Masse,E. (2011) Small RNA-induced mRNA degradation achieved through both translation block and activated cleavage. *Genes Dev.*, **25**, 385–396.

32. Wright,P.R., Georg,J., Mann,M., Sorescu,D.A., Richter,A.S., Lott,S., Kleinkauf,R., Hess,W.R. and Backofen,R. (2014) CopraRNA and IntaRNA: predicting small RNA targets, networks and interaction domains. *Nucleic Acids Res.*, **42**, W119–W123.

33. Chao,Y., Li,L., Girodat,D., Forstner,K.U., Said,N., Corcoran,C., Smiga,M., Papenfort,K., Reinhardt,R., Wieden,H.J. et al. (2017) In vivo cleavage map illuminates the central role of RNase E in coding and non-coding RNA pathways. *Mol. Cell*, **65**, 39–51.

34. Schu,D.J., Zhang,A., Gottesman,S. and Storz,G. (2015) Alternative Hfq-sRNA interaction modes dictate alternative mRNA recognition. *EMBO J.*, **34**, 2557–2573.

35. Desnoyers,G. and Masse,E. (2012) Noncanonical repression of translation initiation through small RNA recruitment of the RNA chaperone Hfq. *Genes Dev.*, **26**, 726–739.

36. Zuker,M. (2003) Mfold web server for nucleic acid folding and hybridization prediction. *Nucleic Acids Res.*, **31**, 3406–3415.

37. Darty,K., Denise,A. and Ponty,Y. (2009) VARNA: interactive drawing and editing of the RNA secondary structure. *Bioinformatics*, **25**, 1974–1975.

38. Wolfe,A.J., Parikh,N., Lima,B.P. and Zemaitaitis,B. (2008) Signal integration by the two-component signal transduction response regulator CpxR. *J. Bacteriol.*, **190**, 2314–2322.

39. Ikeda,Y., Yagi,M., Morita,T. and Aiba,H. (2011) Hfq binding at RhlB-recognition region of RNase E is crucial for the rapid degradation of target mRNAs mediated by sRNAs in Escherichia coli. *Mol. Microbiol.*, **79**, 419–432.

40. Peterman,N., Lavi-Itzkovitz,A. and Levine,E. (2014) Large-scale mapping of sequence-function relations in small regulatory RNAs reveals plasticity and modularity. *Nucleic Acids Res.*, **42**, 12177–12188.

41. Rutherford,S.T., Valastyan,J.S., Taillefumier,T., Wingreen,N.S. and Bassler,B.L. (2015) Comprehensive analysis reveals how single nucleotides contribute to noncoding RNA function in bacterial quorum sensing. *Proc. Natl. Acad. Sci. U.S.A.*, **112**, E6038–E6047.

42. Moller,T., Franch,T., Udesen,C., Gerdes,K. and Valentin-Hansen,P. (2002) Spot 42 RNA mediates discoordinate expression of the E. coli galactose operon. *Genes Dev.*, **16**, 1696–1706.

43. Chabelskaya,S., Gaillot,O. and Felden,B. (2010) A Staphylococcus aureus small RNA is required for bacterial virulence and regulates the expression of an immune-evasion molecule. *PLoS Pathog*, **6**, e1000927.

44. Eyraud,A., Tattevin,P., Chabelskaya,S. and Felden,B. (2014) A small RNA controls a protein regulator involved in antibiotic resistance in Staphylococcus aureus. *Nucleic Acids Res.*, **42**, 4892–4905.

45. Bos,J., Duverger,Y., Thouvenot,B., Chiaruttini,C., Branlant,C., Springer,M., Charpentier,B. and Barras,F. (2013) The sRNA RyhB regulates the synthesis of the Escherichia coli methionine sulfoxide reductase MsrB but not MsrA. *PLoS One*, **8**, e63647.

46. Bobrovskyy,M. and Vanderpool,C.K. (2016) Diverse mechanisms of post-transcriptional repression by the small RNA regulator of glucose-phosphate stress. *Mol. Microbiol.*, **99**, 254–273.

47. Corcoran,C.P., Podkaminski,D., Papenfort,K., Urban,J.H., Hinton,J.C. and Vogel,J. (2012) Superfolder GFP reporters validate diverse new mRNA targets of the classic porin regulator, MicF RNA. *Mol. Microbiol.*, **84**, 428–445.

48. Chao,Y. and Vogel,J. (2016) A 3′ UTR-derived small RNA provides the regulatory noncoding arm of the inner membrane stress response. *Mol. Cell*, **61**, 352–363.

49. Coyer,J., Andersen,J., Forst,S.A., Inouye,M. and Delihas,N. (1990) micF RNA in ompB mutants of Escherichia coli: different pathways regulate micF RNA levels in response to osmolarity and temperature change. *J. Bacteriol.*, **172**, 4143–4150.

50. Hommais,F., Krin,E., Coppee,J.Y., Lacroix,C., Yeramian,E., Danchin,A. and Bertin,P. (2004) GadE (YhiE): a novel activator involved in the response to acid environment in Escherichia coli. *Microbiology*, **150**, 61–72.

51. Tucker,D.L., Tucker,N. and Conway,T. (2002) Gene expression profiling of the pH response in Escherichia coli. *J. Bacteriol.*, **184**, 6551–6558.

52. Peng,C.A., Oliver,M.J. and Wood,A.J. (2005) Is the Rehydrin TrDr3 from Tortula ruralis associated with tolerance to cold, salinity, and reduced pH? Physiological evaluation of the TrDr3-orthologue, HdeD from Escherichia coli in response to abiotic stress. *Plant Biol. (Stuttg.)*, **7**, 315–320.

53. Wyborn,N.R., Messenger,S.L., Henderson,R.A., Sawers,G., Roberts,R.E., Attwood,M.M. and Green,J. (2002) Expression of the Escherichia coli yfiD gene responds to intracellular pH and reduces the accumulation of acidic metabolic end products. *Microbiology*, **148**, 1015–1026.

54. Padan,E., Bibi,E., Ito,M. and Krulwich,T.A. (2005) Alkaline pH homeostasis in bacteria: new insights. *Biochim. Biophys. Acta*, **1717**, 67–88.

55. Kim,D., Hong,J.S., Qiu,Y., Nagarajan,H., Seo,J.H., Cho,B.K., Tsai,S.F. and Palsson,B.O. (2012) Comparative analysis of regulatory elements between Escherichia coli and Klebsiella pneumoniae by genome-wide transcription start site profiling. *PLoS Genet.*, **8**, e1002867.

56. Lalaouna,D. and Masse,E. (2016) The spectrum of activity of the small RNA DsrA: not so narrow after all. *Curr. Genet.*, **62**, 261–264.

57. Soper,T.J. and Woodson,S.A. (2008) The rpoS mRNA leader recruits Hfq to facilitate annealing with DsrA sRNA. *RNA*, **14**, 1907–1917.

58. Mika,F. and Hengge,R. (2014) Small RNAs in the control of RpoS, CsgD, and biofilm architecture of Escherichia coli. *RNA Biol.*, **11**, 494–507.

59. Bordeau,V. and Felden,B. (2014) Curli synthesis and biofilm formation in enteric bacteria are controlled by a dynamic small RNA module made up of a pseudoknot assisted by an RNA chaperone. *Nucleic Acids Res.*, **42**, 4682–4696.

60. Saliba,A.E., S,C.S. and Vogel,J. (2017) New RNA-seq approaches for the study of bacterial pathogens. *Curr. Opin. Microbiol.*, **35**, 78–87.

61. Holmqvist,E., Wright,P.R., Li,L., Bischler,T., Barquist,L., Reinhardt,R., Backofen,R. and Vogel,J. (2016) Global RNA recognition patterns of post-transcriptional regulators Hfq and CsrA revealed by UV crosslinking in vivo. *EMBO J.*, **35**, 991–1011.

62. Chao,Y., Papenfort,K., Reinhardt,R., Sharma,C.M. and Vogel,J. (2012) An atlas of Hfq-bound transcripts reveals 3′ UTRs as a genomic reservoir of regulatory small RNAs. *EMBO J.*, **31**, 4005–4019.

63. Melamed,S., Peer,A., Faigenbaum-Romm,R., Gatt,Y.E., Reiss,N., Bar,A., Altuvia,Y., Argaman,L. and Margalit,H. (2016) Global mapping of small RNA-target interactions in bacteria. *Mol. Cell*, **63**, 884–897.

64. Waters,S.A., McAteer,S.P., Kudla,G., Pang,I., Deshpande,N.P., Amos,T.G., Leong,K.W., Wilkins,M.R., Strugnell,R., Gally,D.L. *et al.* (2017) Small RNA interactome of pathogenic E. coli revealed through crosslinking of RNase E. *EMBO J.*, **36**, 374–387.

65. Lalaouna,D. and Masse,E. (2015) Identification of sRNA interacting with a transcript of interest using MS2-affinity purification coupled with RNA sequencing (MAPS) technology. *Genomics Data*, **5**, 136–138.

66. Han,K., Tjaden,B. and Lory,S. (2016) GRIL-seq provides a method for identifying direct targets of bacterial small regulatory RNA by in vivo proximity ligation. *Nat. Microbiol*, **2**, 16239.